Morphology development in toughened aliphatic polyamides

B. Majumdar*, H. Keskkula and D. R. Paul†
Department of Chemical Engineering and Center for Polymer Research, University of Texas at Austin, Austin, TX 78712, USA
(Received 16 April 1993; revised 9 August 1993)

The morphology of binary blends of a maleated triblock copolymer (with an ethylene/butene midblock and styrene endblocks, SEBS-*g*-MA) with a series of nylon materials (nylon 4,6, nylon 6,9, nylon 6,10, nylon 6,12, nylon 11, nylon 12 and nylon 12,12) was investigated and the results compared with previous work for nylon 6 and nylon 6,6. The nylon *x* materials (nylon 11 and nylon 12) yielded small, regular particles similar to that observed in nylon 6. These nylons have one amine endgroup per molecule and are only capable of end-grafting. The nylon *x,y* materials, on the other hand, led to much larger and more complex-shaped particles; their size decreased as the aliphatic content of the nylon increased. These polyamides contain a certain fraction of molecules with two amine endgroups and are capable of forming loops or crosslinks which dramatically affect the morphology generation in a single-screw extruder. The results further revealed that the large particles are formed because of the failure of the single-screw extruder to break them into smaller ones rather than by increased coalescence. There is evidence that thickness of the interface influences both the particle size and the extent of reaction in these blends as described.

(Keywords: blends; polyamides; block copolymers)

INTRODUCTION

The toughening of polyamides with suitable elastomeric materials has been the subject of a number of recent papers[1–7]. Since the commercial introduction of supertough nylon[8,9], various attempts have been made to gain deeper insights into the chemistry and morphology related to the toughening process in polyamides. In most cases, the elastomeric phase is grafted with a functional monomer (e.g. maleic anhydride) that reacts readily with the polyamide during melt processing, providing the required adhesion between the two phases and controlling the dispersed rubber particle morphology. For nylon 6 and nylon 6,6, it has been demonstrated that the rubber particle size must be below a critical diameter of approximately 1 μm to achieve supertoughness[4–12]. It has also been argued that the true critical dimension is the interparticle distance rather than the particle size[13]. More recent work has revealed a critical lower limit on rubber particle size ($\sim$0.2 μm) below which supertoughness is not achieved for nylon 6[4,7].

Numerous factors affect the generation of morphology in such systems, including interfacial tension[14], relative viscosities between the two phases[15–17], mixing intensity and other processing parameters[16,17], concentration of the reactive polyamide endgroups[18] etc.

Our previous work[4–6] used hydrogenated styrene–butadiene–styrene triblock elastomers whose midblocks resemble ethylene/butene copolymers, designated SEBS, and a version grafted with maleic anhydride, SEBS-*g*-MA. It has been reported that nylon 6,6 could be toughened by blending (in a single-screw extruder) with SEBS-*g*-MA alone[1–3,5], while a combination of the maleated and the unmaleated elastomer was required for toughening nylon 6[1–4]. Transmission electron microscopy (TEM) photomicrographs revealed that the particles of functionalized elastomer in the blends with nylon 6,6 were much more complex in nature than the very small, spherical particles produced in nylon 6. These dramatic differences were attributed to a fundamental difference in the chemical nature of these polyamides, i.e. their monofunctional *versus* difunctional character in terms of reactions with anhydrides[5].

More recently, it has been shown that blends of SEBS-*g*-MA with other monofunctional polyamides, nylon 11 and nylon 12, give small, regular-shaped rubber particles similar to those observed for nylon 6, while blends with nylon 12,12 give large complex particles similar to those formed with nylon 6,6[6]. It was also shown that addition of 10% nylon 6,6, poly(*m*-xylene adipamide), (MXD6), or nylon 12,12 to nylon 6 (under conditions that cause interchange reactions) leads to rubber particle enlargement and toughening, while addition of nylon 11 and nylon 12 does not.

The purpose of this paper is to explore further the differences in morphology of blends of SEBS-*g*-MA with a range of aliphatic polyamides including both nylon *x* and nylon *x,y* types. The aliphatic character specified by the ratio of methylene units per amide linkage in the repeat unit, or $CH_2/NHCO$, was varied from 4 to 11. An accompanying paper addresses issues related to the mechanical properties of these blends[19]. Very little work has been reported on the toughening of polyamides other than nylon 6 and nylon 6,6.

* Present address: Department of Chemical Engineering and Material Science, University of Minnesota, 151 Amundson Hall, 421 Washington Avenue SE, Minneapolis, MN 55455-0132, USA
† To whom correspondence should be addressed

0032-3861/94/07/1386–13

Nylon 6 simply polymerized from caprolactam yields chains with only one amine endgroup that can react with maleated rubber particles. However, nylon 6,6 as usually prepared has a certain fraction of chains having two amine endgroups. Thus, with respect to reaction with anhydride units, these nylon 6 chains are monofunctional, i.e. only one end of each chain is reactive. The nylon 6,6 chains with amine groups on both ends are, thus, difunctional, which can lead to formation of loops or bridges, i.e. crosslinking-like effects, *versus* the simple endgrafting that occurs for nylon 6.

All of the blends described previously and in this paper were prepared using a single-screw extruder. A future paper will show the effects on morphology and toughening of using a twin-screw extruder that provides more intensive mixing. Other work in progress will deal more thoroughly with rheological issues as well as nylon 6 materials with modified endgroup structures.

BACKGROUND

Morphology generation in two-phase blends is usually discussed in terms of a balance between fluid drop break-up and coalescence. The final product has the morphological structure that is captured when the blend is solidified. According to the Taylor theory[20,21] drop break-up will occur in a shear field when the ratio of the viscous to interfacial tension forces exceeds a critical value that depends on the relative viscosities of the two phases. Although this theory applies strictly only to Newtonian flow, it has been utilized as a common framework for explaining dispersion phenomena for complex viscoelastic flow-fields in polymer blends. Based on the above principles, correlations of the following form have been developed[15,16]:

$$\eta_m G d/\gamma = F(\eta_d/\eta_m) \tag{1}$$

where γ is the interfacial tension, G the shear rate, η_m the viscosity of the matrix phase and η_d the viscosity of the dispersed phase. Hence, if all other factors are the same, the particle diameter, d, will be directly proportional to the interfacial tension, that is

$$d \sim \gamma \tag{2}$$

Attempts have also been made to account for the phenomenon of coalescence as the dispersed particles collide during processing based on Smoluchowski's theory for aqueous colloid suspensions[22,23]. These theories in general predict an increase in phase size with dispersed-phase concentration owing to the increased probability of collisions as the number density of particles increases[24–26].

It is clear from equation (2) that the interfacial tension between the two phases plays an important role in determining particle size in polymer blends. In the recent past, a number of attempts have been made to quantify the interfacial tension between the phases in polymer blends using both theoretical[27–30] and experimental[31–35] approaches. A model proposed by Helfand[27–29], based on a mean-field theory, has been extensively utilized for quantitatively characterizing the polymer–polymer interface[27,31,36]. This theory relates the interfacial thickness, λ, and the interfacial tension, γ, to the Flory–Huggins interaction parameter as follows:

$$\lambda = \left(\frac{2RT}{B}\right)^{1/2} (\beta_A^2 + \beta_B^2)^{1/2} \tag{3}$$

$$\gamma = \frac{(RTB)^{1/2}}{2}[\beta_A + \beta_B]\left[1 + \frac{1}{3}\frac{(\beta_A - \beta_B)^2}{(\beta_A + \beta_B)^2}\right] \tag{4}$$

where

$$\beta_i = \left(\frac{\rho_i \langle r_i^2 \rangle}{6M_i}\right) \tag{5}$$

In these expressions $\langle r_i^2 \rangle$ is the mean square end-to-end distance[37] and M_i is the average molecular weight for component i. The interaction energy density, B, for the A–B pair is used instead of the conventional χ ($= BV_{ref}/RT$) since this avoids the definition of the arbitrary reference volume, V_{ref}. In general, Helfand's model predicts interfacial tension values that are in close agreement with experimental results for a number of systems[27,31]. More recently, several authors have attempted to develop theoretical models based on mean-field theory to describe how the presence of block copolymers[38–42] at the interface between homopolymer melts reduces the interfacial tension and broadens the interfacial zone.

At present, there is no single theoretical model which can adequately describe all the physical aspects of a reactive interface in the case of reactive compatibilization where block or graft copolymers are generated *in situ* at the interface. In the classical view of compatibilization[43–49], reactions at the interface lead to a decrease in the interfacial tension and some stabilization against coalescence. In our recent work it has been demonstrated that the particle size can be varied by over two orders of magnitude by graft copolymer formation at the interface. Such large changes in particle size only partially reflect the reduction in interfacial tension; steric hindrances against coalescence caused by such graft chains can be an even more important factor influencing particle size[25,50]. More recently, it has been suggested that the topology of grafting plays an important role in determining the final morphology of the blend[5,6]. In the case of the blends of SEBS-*g*-MA with difunctional nylons, complex particles with evidence of considerable occlusions of the matrix material were generated. These observations have been attributed to the 'crosslinking'-type effects developed through the two particle attachments per chain possible in difunctional polyamides. For monofunctional polyamides, on the other hand, one-point attachments apparently lead to small, spherical particles[1–4].

The extent of chemical reaction at the interface depends on the thickness of the interfacial zone generated between the two phases. A more favourable polymer–polymer interaction energy (lower B or χ) promotes a broadening of the interfacial zone between the two phases as predicted from equation (3). A more diffuse interface enhances the probability that functional groups can approach each other and react[46,48] leading to a higher extent of reaction.

EXPERIMENTAL

Table 1 summarizes pertinent information about the various materials used in this study. All polyamide materials were dried at 80°C for at least 12 h in a vacuum oven to remove sorbed water before processing. The two triblock copolymers employed as rubbers have styrene endblocks and a hydrogenated butadiene midblock resembling an ethylene/butene copolymer. The non-reactive elastomer is designated SEBS while the maleated version, containing 1.84% by weight of grafted maleic

Table 1 Polymers used in this study

Polymer	Commercial designation	$\bar{M}_n$ (× 1000)	Endgroup content (μeq g^{-1})		Relative melt viscosity[a]	Source
			NH_2	COOH		
Nylon 6	Capron 8207F	25	40.0	40.0	1.0	Allied Signal Inc.
Nylon 6,6	Zytel 101	17	46.4	NA	1.4[b]	E.I. du Pont Co.
Nylon 11-A	BMNO TL	25[d]	46.4	43.4	2.4	Atochem Inc.
Nylon 11-B	BESNO TL	NA	NA	NA	0.8	Atochem Inc.
Nylon 11-C	BESVO	NA	NA	NA	0.3	Atochem Inc.
Nylon 12-A	AESNO TL	16[d]	44.7	50.5	0.5	Atochem Inc.
Nylon 12-B	A M N O	NA	NA	NA	3.9	Atochem Inc.
Nylon 12,12	Zytel 40-401	NA	46.0	47.6	1.5	E.I. du Pont Co.
Nylon 6,12	Zytel 158 L	NA	43.8	41.7	1.8	E.I. du Pont Co.
Nylon 6,10	Nylon 6,10	25[d]	32.6	NA	0.7[b]	Aldrich Chemical Co.
Nylon 6,9	Nylon 6,9	28[d]	33.9	NA	1.2[b]	Aldrich Chemical Co.
Nylon 4,6	Stanyl	22[d]	19.8	NA	1.0[c]	DSM
(SEBS)	Kraton G 1652	Styrene block = 7 EB block = 37.5	–	–	0.56	Shell Chemical Co.
(SEBS-*g*-MA) 1.84% maleic anhydride	Kraton 1901X	NA	–	–	1.0	Shell Chemical Co.

[a,b,c] Brabender torque of SEBS-*g*-MA relative to the polyamide at 240°C at 60 rev min^{-1} after 10 min at [a] 240°C; [b] 280°C; [c] 310°C
[d] From ref. 72
NA, not available

anhydride along the olefinic midblock, is designated SEBS-*g*-MA.

For rheological characterization, the various polymers were mixed in a Brabender Plasticorder with a 50 ml mixing head and standard rotors, while the torque was recorded. All tests were made at 60 rev min^{-1} and 240°C, unless otherwise specified.

The various polyamides were blended with SEBS and SEBS-*g*-MA by a single pass through a 2.54 cm Killion single-screw extruder ($L/D = 30$) at 240°C (in most cases). Extruded blends were moulded into standard Izod bars (ASTM D256) and tensile bars (ASTM D638 type I) of 0.318 cm thickness using an Arburg Allrounder screw injection-moulding machine.

Blend morphology was determined by TEM. Samples were cryogenically microtomed from Izod bars perpendicular to the flow direction using a diamond knife. Two different staining procedures were employed to generate contrast between the phases. In most cases, the rubber was stained with ruthenium tetroxide[51–54]. A 2% solution of phosphotungstic acid (PTA) was also used to stain the polyamide matrix, which is especially useful for revealing any occlusions of polyamide material inside the rubber phase[55–59]. A JOEL transmission electron microscope (JEM-1200EX) operated at an accelerating voltage of 120 kV was used to view and photograph these sections, which are only of the order of nanometres in thickness. A semi-automatic digital image analysis technique was employed to determine the effective diameters of the dispersed phase from the TEM photomicrographs using NIH Image® software. For complex shapes of the rubber phase, the diameter assigned to each particle (including any occluded polyamide) was the average of its longest dimension and its dimension perpendicular to its major axis[6]. No corrections were attempted to convert these apparent particle diameters into true sizes since the methods stated in the literature[60–63] are not applicable for complex shapes.

The extent of reaction in these blends was measured by amine group titration of the final blend and the pure nylon. The extent of reaction was calculated assuming that the dominant reaction is of an amine end with an anhydride unit to give an imide linkage[10]. A detailed description of the measurement technique will be provided elsewhere.

RHEOLOGY

Brabender torque rheometry has been used to characterize the melt flow behaviour of the individual components (see *Table 1*) of the blend and for obtaining an indication of grafting reactions during blending[64–67]. After an initial transient period, all pure components and their blends reached a constant torque value. The value after 10 min is thus used hereafter as a means of characterizing these materials. This torque is proportional to the melt viscosity of the melt at the effective shear rate in the mixer, which approximates that in the single-screw extruder. *Figure 1* shows the torque at 10 min over the entire spectrum of composition for SEBS-*g*-MA blended with four polyamides. For nylon 12 and nylon 12,12, there is a strong peak maximum at around 20% SEBS-*g*-MA. Interestingly, nylon 6 also displays a maximum close to this composition[4]. On the other hand, nylon 11 shows a sharp peak at 80% rubber while nylon 6,12 shows a much broader maximum. It is beyond the scope of this work to provide a detailed interpretation of the differences in the torque responses for blends of various polyamides with the reactive rubber. A combination of numerous factors including differences in the relative viscosities between the two phases, endgroup concentrations of the polyamides, interfacial tensions, etc. are probably involved.

The melt viscosities of the various polyamides relative to that of SEBS-*g*-MA, shown in *Table 1*, have been computed by calculating the ratios of the Brabender

torque values at 60 rev min^{-1} after 10 min. The multiple points for nylon 11 and nylon 12 represent different molecular weight grades.

For multiphase blends, morphology generation can be explained in terms of a balance between fluid drop break-up and phase coalescence. The viscosity of the dispersed phase relative to that of the matrix is a critical parameter in determining morphology for both reactive and non-reactive systems[15–17]. In the latter part of this work, this ratio has been fixed at as near as possible to unity while investigating variations caused by other parameters.

EFFECT OF CHEMICAL FUNCTIONALITY ON MORPHOLOGY

The objective of this work is to examine how the endgroup and repeat unit structure of polyamides influences the morphology of their blends with a maleated elastomer. Previous studies demonstrated large differences in the morphology of blends based on nylon 6 and nylon 6,6 that were attributed to the monofunctional *versus* difunctional character of these materials in terms of reactions with anhydride groups. Based on this hypothesis, it was postulated that blends of SEBS-*g*-MA with other monofunctional polyamides (nylon *x*) will yield regular spherical particles similar to those observed in nylon 6, while blends with difunctional polyamides (nylon *x*,*y*) should lead to larger particles of more complex character.

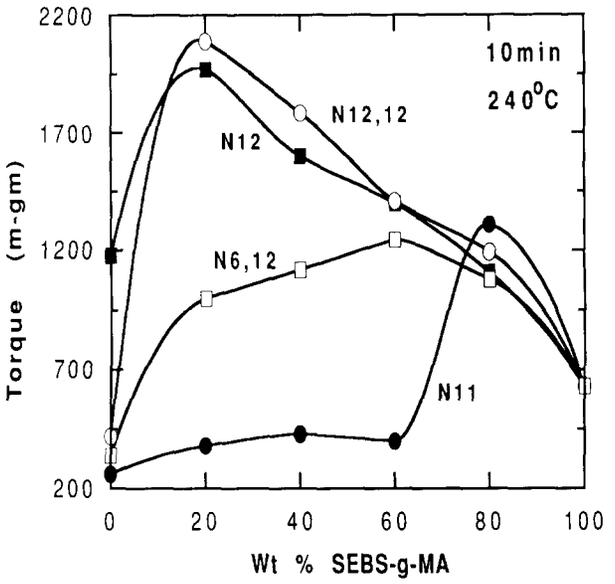

Figure 1 Brabender torques for blends of various polyamides with SEBS-*g*-MA after 10 min at 240°C and 60 rev min^{-1}

TEM photomicrographs of blends of nylon 11-B and nylon 12-A with SEBS-*g*-MA are shown in *Figure 2*. The polyamide matrix in these TEM photomicrographs was stained with PTA to generate sharp contrast between the two phases. Small, nearly spherical rubber particles similar to those generated with nylon 6[4] are seen.

Figures 3–6 show TEM photomicrographs of blends of nylon 4,6, nylon 6,6, nylon 6,9, nylon 6,10, nylon 6,12 and nylon 12,12 with SEBS-*g*-MA. It is evident that these polyamides generate particles that are much larger and more complex in shape than those in nylon 6, nylon 11 and nylon 12. These results are clearly distinguished by the monofunctional or difunctional character, as defined earlier, of the polyamide matrices. For some blends, TEM photomicrographs obtained following two different staining techniques are shown. *Figure 3a* shows the morphology for a nylon 4,6 blend where the rubber was stained with RuO_4. Extremely large particles with considerable occlusions of the polyamide within the rubber are seen. *Figure 3b* shows the morphology of the same blend where the polyamide phase was stained with PTA. The occluded nylon material (stained black) can be clearly observed within the rubber particles in this photomicrograph. *Figure 4* compares the morphology generated in nylon 6,6 using RuO_4 staining of the rubber (*Figure 4a*) and PTA staining of the polyamide matrix (*Figure 4b*). Both stains reveal the complex shapes of the rubber particles; however, PTA staining most clearly reveals the fine occluded structures of nylon 6,6 inside the rubber particles. *Figure 5* shows, using the two

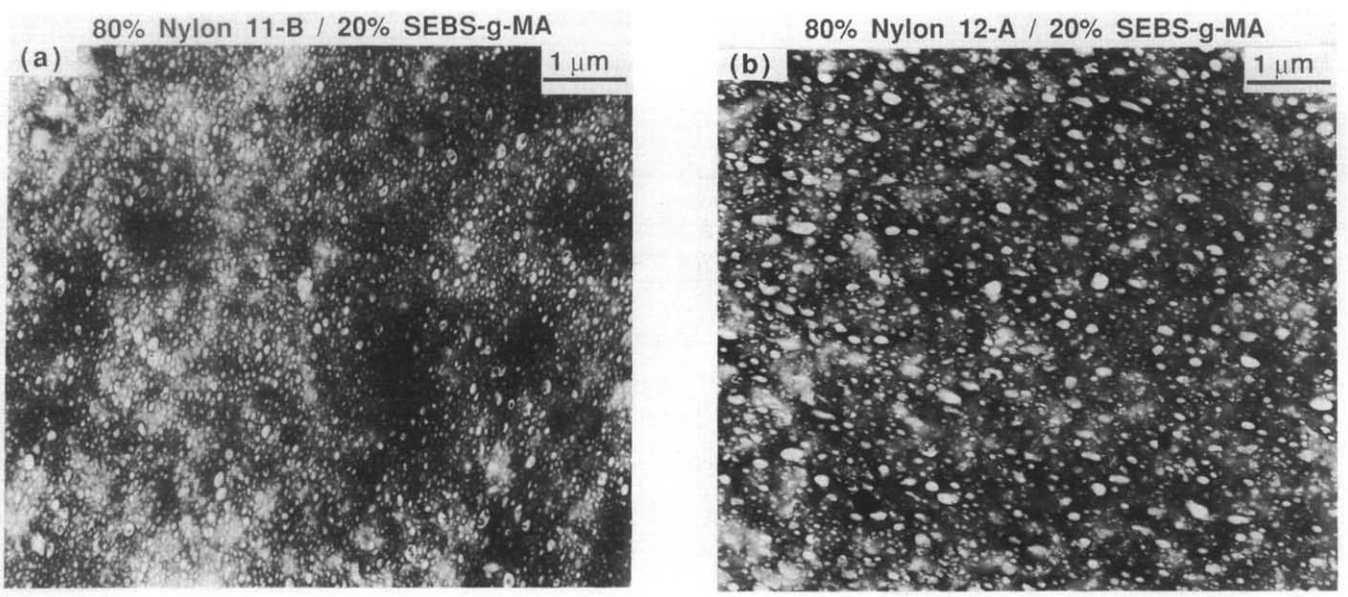

Figure 2 TEM photomicrographs of blends containing 20% SEBS-*g*-MA and 80% (a) nylon 11-B and (b) nylon 12-A. The nylon phase has been stained with PTA in both cases

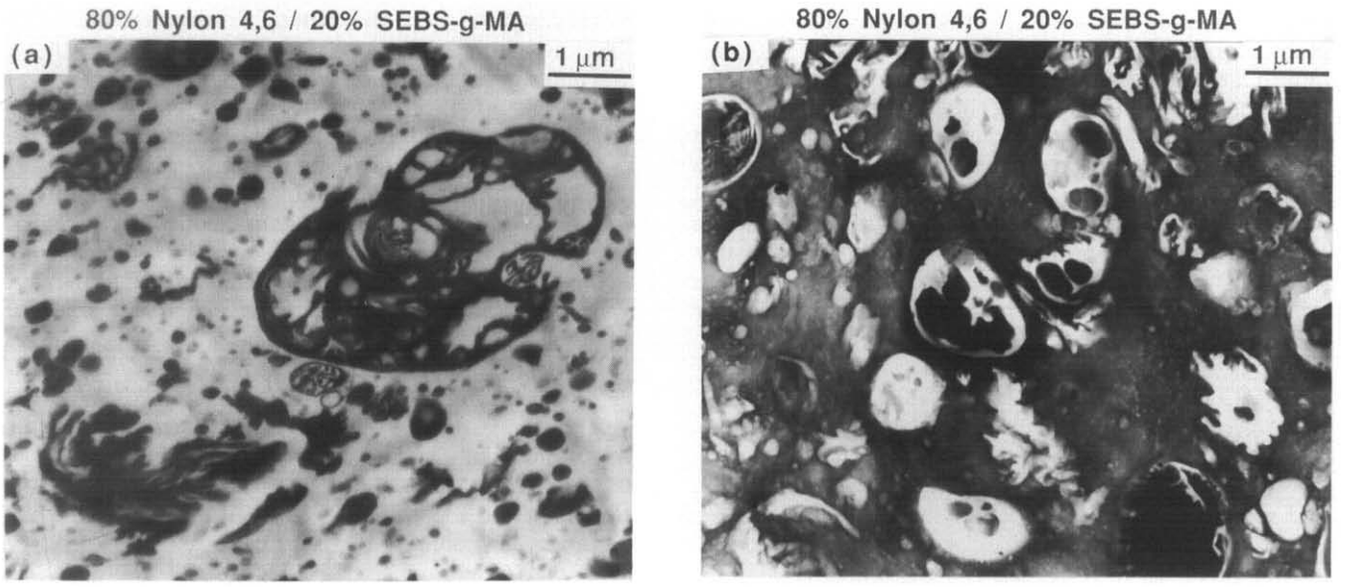

Figure 3 TEM photomicrographs of 80% nylon 4,6/20% SEBS-*g*-MA blend in which (a) the rubber phase has been stained with RuO_4 and (b) the nylon phase has been stained with PTA

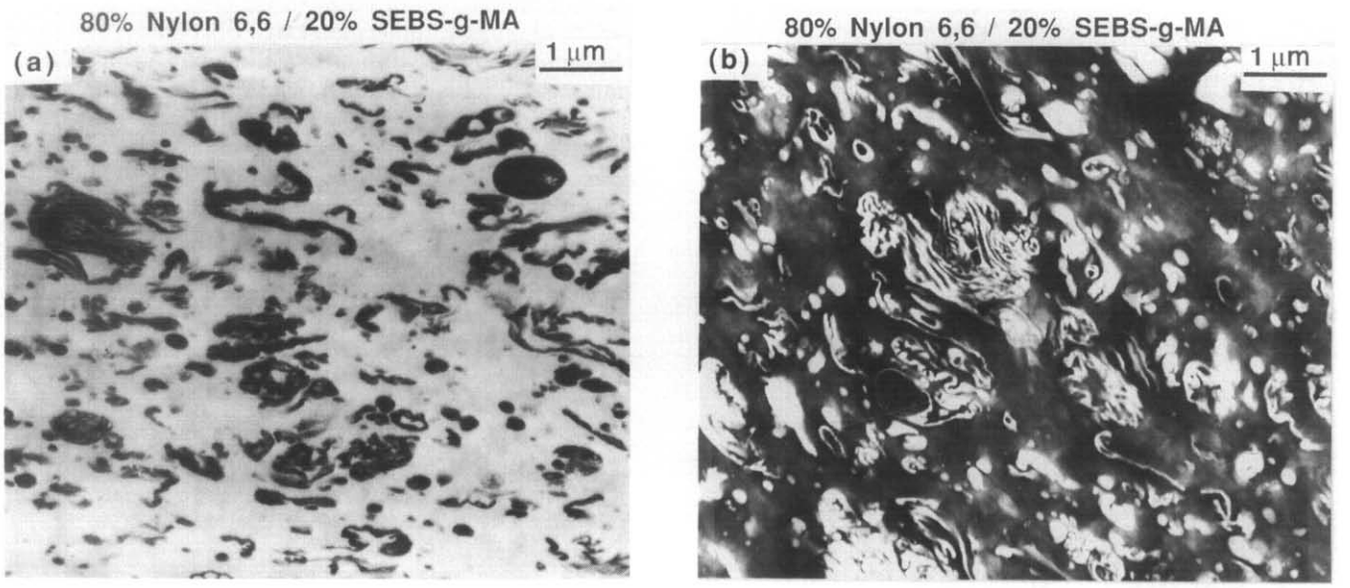

Figure 4 TEM photomicrographs of 80% nylon 6,6/20% SEBS-*g*-MA blend in which (a) the rubber phase has been stained with RuO_4 and (b) the nylon phase has been stained with PTA

techniques, that complex-shaped particles are also generated in nylon 6,9 blends. *Figures 6a, b* and *c* show similar morphological features for blends of SEBS-*g*-MA with nylon 6,10, nylon 6,12 and nylon 12,12, respectively. However, there is a significant reduction in the particle size as the aliphatic character, i.e. the CH_2/NHCO ratio, of the polyamide is increased.

For all the blends described above, the viscosity ratio was maintained as close to unity as possible, as shown in *Table 1*. However, for nylon 11 and nylon 12, use of different molecular weight grades allowed a brief investigation of the effect of the viscosity ratio on the morphology of their blends with SEBS-*g*-MA. *Table 2* shows the particle size determined from TEM photomicrographs for the different grades of nylon 11 and 12. For nylon 12, a smaller particle size was observed for the grade whose viscosity was more closely matched with the rubber phase. On the other hand, for nylon 11, among the three different grades used, the particle size continues to decrease as the relative melt viscosity between the two phases is lowered. A TEM photomicrograph for the blend based on the lowest molecular weight nylon 11 (nylon 11-A) is shown in *Figure 6d*. Although the general character of the rubber particles is similar to that observed in the case of nylon 11-B, the large mismatch in the viscosity ratio (2.4) for nylon 11-A leads to a significant enlargement and broader distribution ($\bar{d}_w/\bar{d}_n = 1.15$) of particle diameters than observed for nylon 11-B ($\bar{d}_w/\bar{d}_n = 1.06$). In the case of nylon 11-C, which has a viscosity ratio well below 1, no enlargement of particle size is observed (*Table 2*).

Figure 7 summarizes the relationship between the rubber particle diameter and the nature of the polyamide expressed in terms of the hydrocarbon content of

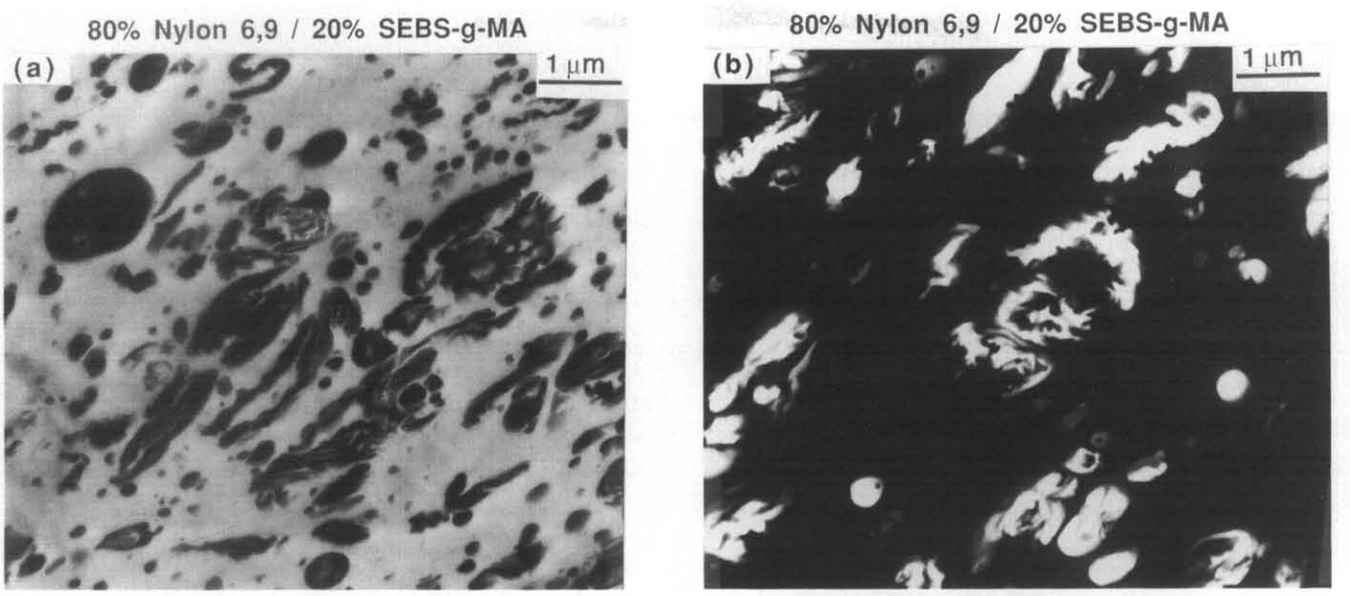

Figure 5 TEM photomicrographs of 80% nylon 6,9/20% SEBS-*g*-MA blend in which (a) the rubber phase has been stained with RuO_4 and (b) the nylon phase has been stained with PTA

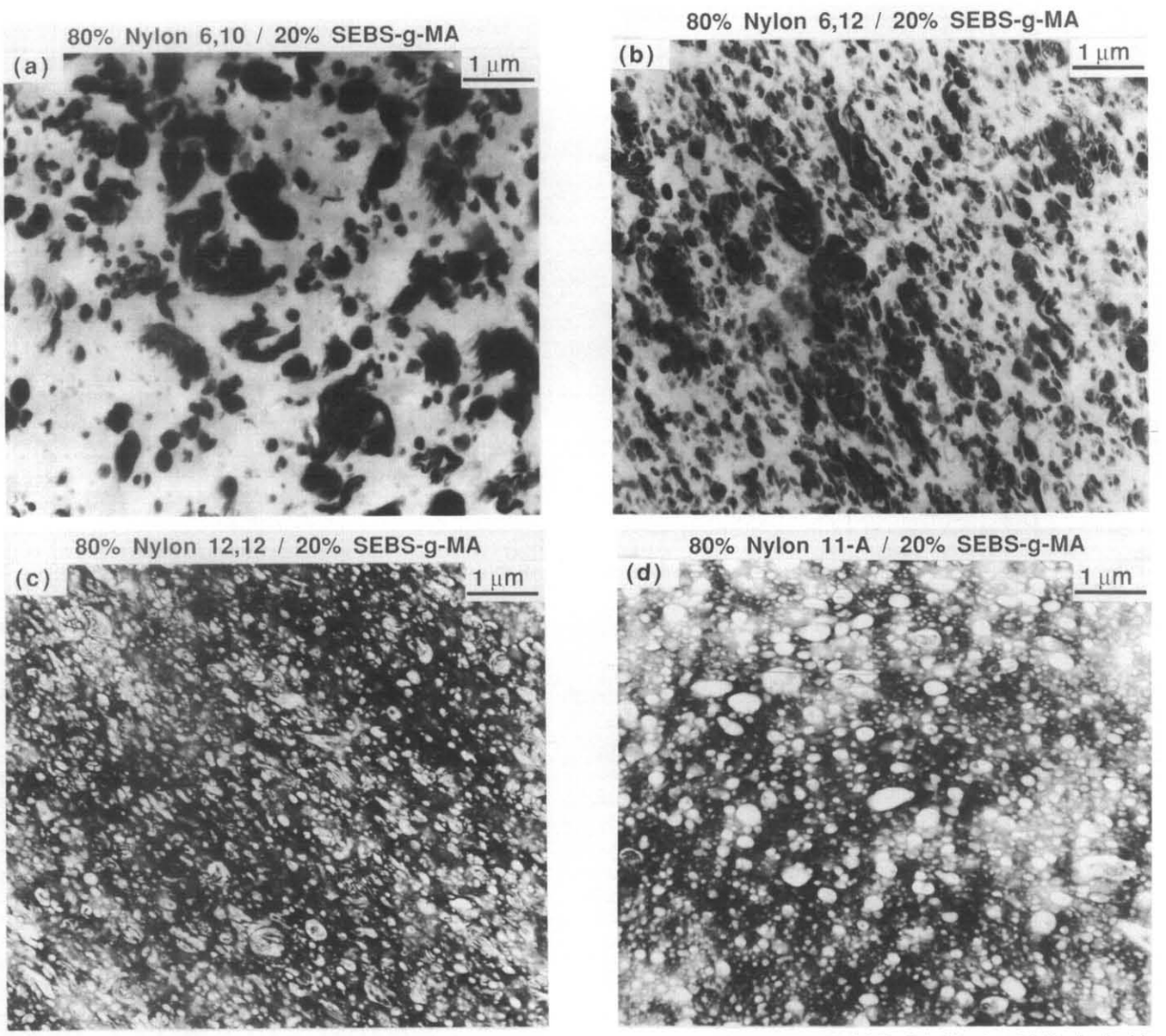

Figure 6 TEM photomicrographs of blends containing 20% SEBS-*g*-MA and 80% (a) nylon 6,10 (stained with RuO_4); (b) nylon 6,12 (stained with RuO_4); (c) nylon 12,12 (stained with PTA); (d) nylon 11-A (stained with PTA)

Table 2 Interfacial parameters, particle size and extent of reaction in polyamide blends

Polyamide	CH_2/NHCO	Volume fraction of amide units ϕ'_2	Estimated nylon/SEBS interfacial thickness λ (Å)	Estimated nylon/SEBS interfacial tension γ (mN m^{-1})	Average SEBS-*g*-MA particle size in nylon blends $\bar{d}_w$ (μm)	$(\lambda/\bar{d}_w) \times 10^3$	Fraction of amine groups reacted x
Nylon 4,6	4	0.2745	25	13.5	1.23	2.1	0.18
Nylon 6,6	5	0.2324	30	11.4	0.98	3.1	0.54
Nylon 6,9	6.5	0.1889	37	9.3	0.79	4.7	0.62
Nylon 6,10	7	0.1778	39	8.8	0.62	6.4	0.67
Nylon 6,12	8	0.1591	44	7.8	0.40	11.1	0.86
Nylon 12,12	11	0.1210	58	5.9	0.21	27.7	0.89
Nylon 6	5	0.2324	30	11.4	0.06	50.5	0.65
Nylon 11-A	10	0.2324	54	6.5	0.15	36.0	NT
Nylon 11-B	10	0.1315	54	6.5	0.09	59.5	NT
Nylon 11-C	10	0.1315	54	6.5	0.05	108.0	NT
Nylon 12-A	11	0.1210	58	5.9	0.10	58.2	0.62
Nylon 12-B	11	0.1210	58	5.9	0.16	36.3	NT

NT, not tested

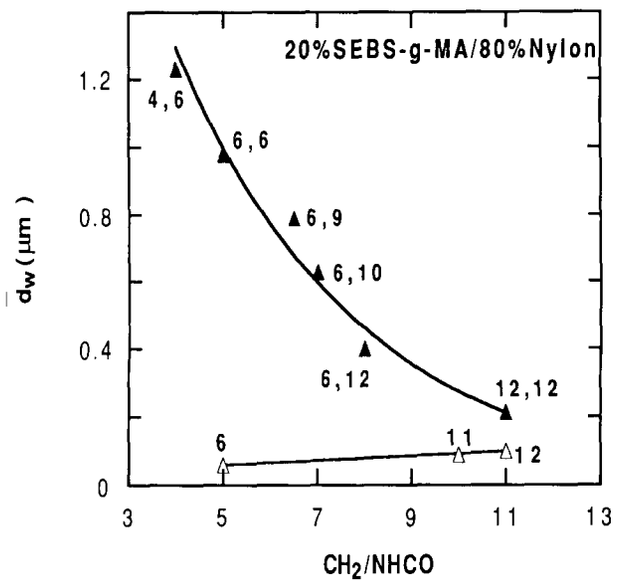

Figure 7 Rubber particle diameter for blends of 20% SEBS-*g*-MA with various polyamides prepared in a single-screw extruder. Polyamides were all selected to have melt viscosities as nearly equal to that of SEBS-*g*-MA as possible

the repeat units, i.e. the CH_2/NHCO ratio. In this plot, the polyamides were selected to have a melt viscosity as close to that of SEBS-*g*-MA as possible. The results clearly divide into two curves depending on the chemical symmetry of the polyamides. The monofunctional polyamides produce regular, spherical particles less than 0.1 μm in diameter showing little variation across the CH_2/NHCO range investigated in this study. The difunctional polyamides, on the other hand, produce larger, complex-shaped particles whose size steadily decreases with increasing CH_2/NHCO ratio. As the CH_2/NHCO ratio is increased, the differences in particle size between the monofunctional and difunctional polyamides tend to diminish. However, even for nylon 12,12, which has the highest CH_2/NHCO ratio among the different difunctional polyamides, the particles have a much more complex shape than for the corresponding monofunctional polyamide, nylon 12 (see *Figures 2* and *6c*). The decrease in particle size as the CH_2/NHCO ratio is increased in the nylon *x,y* series is believed to have its origin in a physical effect described later, whereas the differences in particle size and shapes for nylon *x* and nylon *x,y* (at fixed CH_2/NHCO ratio) are believed to stem from the chemical issue of polyamide amine endgroup configuration.

Morphology development at low rubber concentrations

In dispersed systems, the probability of particle coalescence increases with concentration of particles[22–26] which leads to an increase in average particle size. Thus, by varying the concentration of the dispersed phase over a wide range, it is possible to establish the role that coalescence has in establishing particle size and the nature of the particles. A series of experiments was designed to explore any fundamental differences in the relative influence coalescence has on morphology in blends of maleated rubber with monofunctional or difunctional polyamides. Nylon 6 and nylon 6,6 were blended with SEBS-*g*-MA and its non-reactive precursor, SEBS, over a wide range of rubber concentrations. *Figure 8* shows TEM photomicrographs for blends of nylon 6,6 with SEBS-*g*-MA, containing 1% functionalized rubber, stained by the two different procedures. From both photomicrographs it is clear that extremely complex particles, more than 1 μm in size in some cases, are generated even at this low concentration. *Figure 9* shows a highly magnified view of the remarkably complex nature of the rubber particles generated in the nylon 6,6/SEBS-*g*-MA blend at 1% concentration of the maleated elastomer. *Figure 10* shows TEM photomicrographs for a blend of nylon 6 containing 1% SEBS-*g*-MA. The particles in this blend are in the same size range ($\sim$0.05 μm) as that observed at 20% of the reactive elastomer[1–4]. In some of these TEM photomicrographs, spherulites 2–6 μm in size are also observed.

Figure 11 shows the relationship between the rubber particle size and rubber concentration for nylon 6 and nylon 6,6. In the case of non-reactive rubber, there is a steady increase in the particle size with

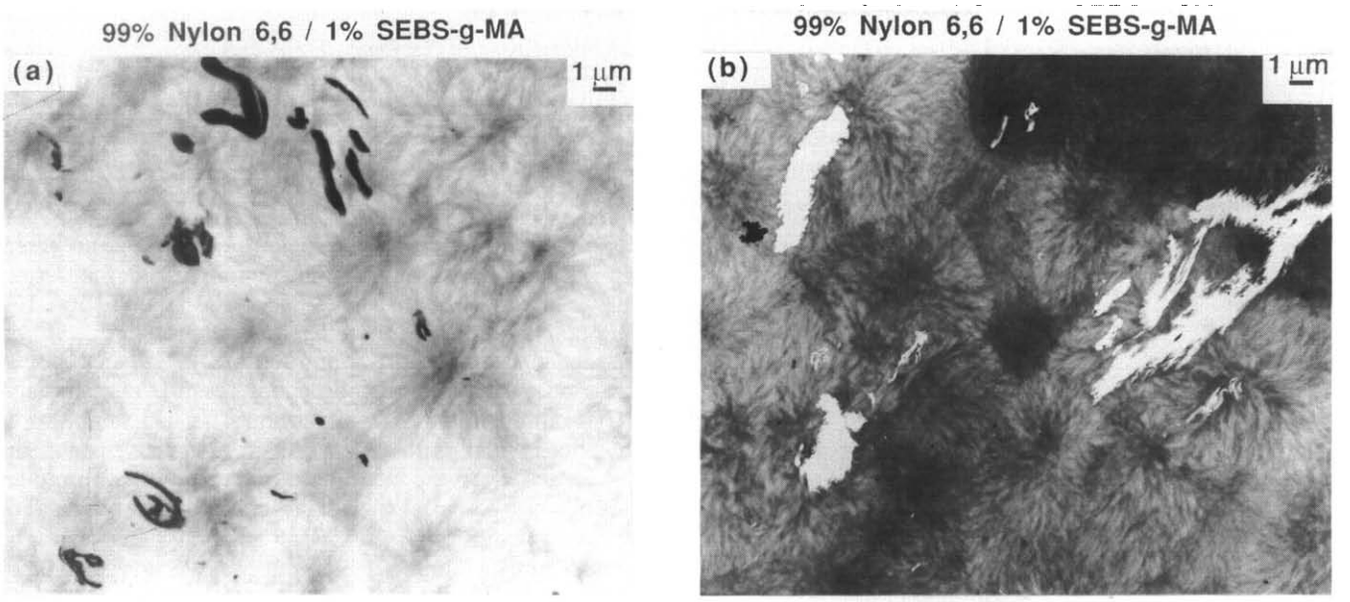

Figure 8 TEM photomicrographs for blend of nylon 6,6 with 1% SEBS-*g*-MA in which (a) the rubber (dark phase) has been stained with RuO_4 and (b) the nylon (dark phase) has been stained with PTA. Note the presence of spherulites in each case

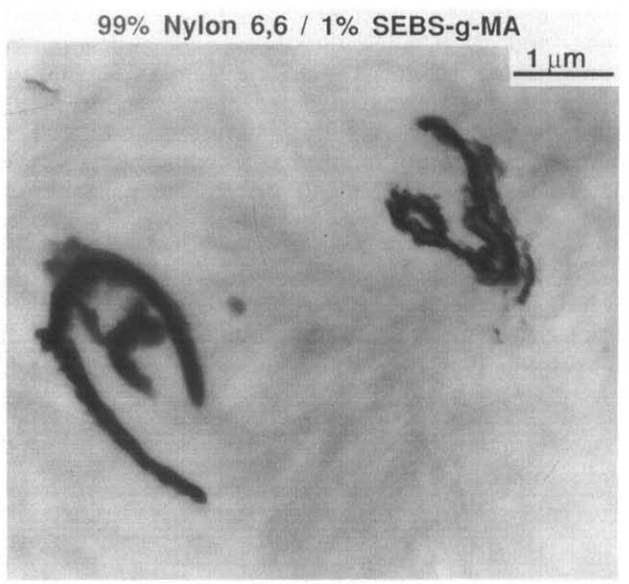

Figure 9 Higher magnification TEM photomicrograph showing the complexity of the rubber particles generated in nylon 6,6 at 1% SEBS-*g*-MA

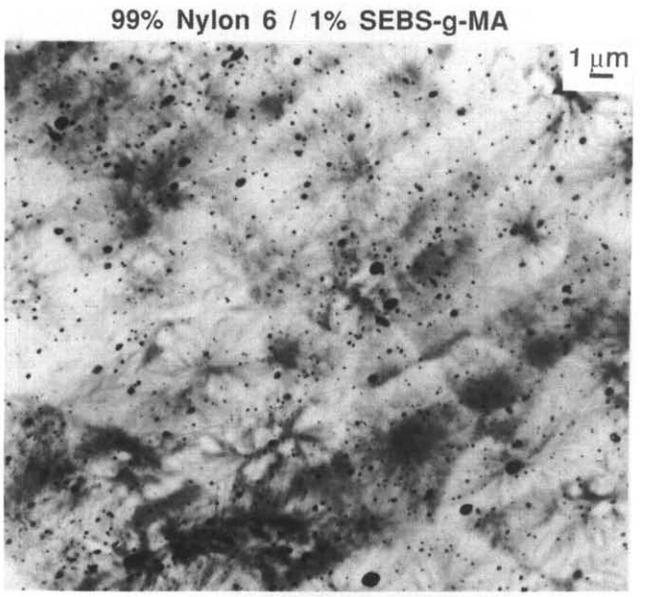

Figure 10 TEM photomicrograph for blend of nylon 6 with 1% SEBS-*g*-MA. The rubber phase (small dark particles) has been stained with RuO_4. Note nylon 6 spherulites

rubber concentration similar to that observed by other investigators[25,50] for a wide variety of blend systems. This trend reflects the increased rate of coalescence, relative to drop break-up rate, as the concentration of particles increases. The model proposed by Tokita[24] quantifies this mechanism. On the other hand, for the reactive rubber, SEBS-*g*-MA, the particle size is essentially constant over the entire range of rubber concentrations for both the polyamides. The fact that practically no change is observed in the SEBS-*g*-MA particle size between 1 and 20% can be attributed to the steric stabilization generated in these cases by the graft copolymer formed at the interface which is evidently very effective in precluding coalescence. A recent study by Willis *et al.*[50] with polystyrene and bromobutyl rubber blends revealed similar results. Even at 1% rubber, the particles of SEBS-*g*-MA in nylon 6,6 are more than an order of magnitude larger than those for nylon 6. This suggests that the dominant reason for the larger particles in nylon 6,6 is the greater difficulty in breaking down these particles, owing to the crosslinking-type effects that stem from its difunctional character, rather than a higher degree of particle coalescence.

Role of the interface

Based on the Taylor theory[20,21] mentioned above, one expects the interfacial tension to be an important factor in determining the size of the dispersed phase in blends. Intuitively, one expects the interfacial tension between a hydrocarbon-type elastomer phase and a polyamide to decrease as the hydrocarbon character of the latter (i.e. the CH_2/NHCO ratio) increases. We believe that

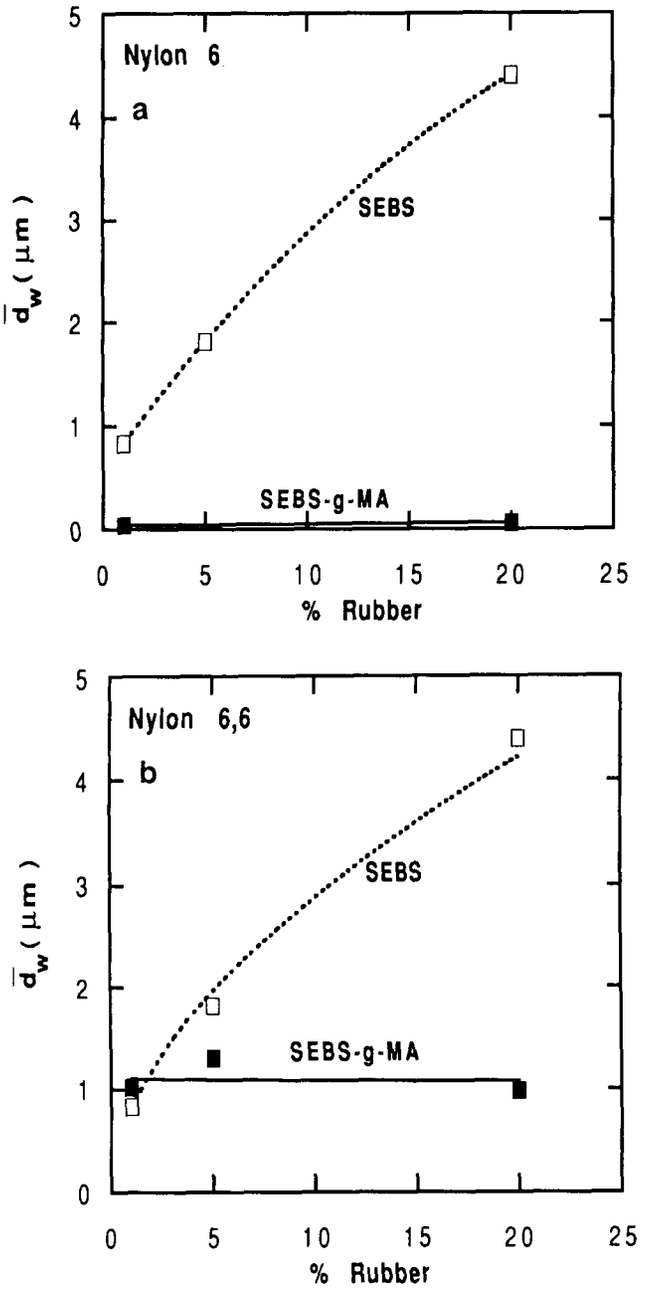

Figure 11 Effect of rubber content on rubber particle size for blends of SEBS and SEBS-*g*-MA with nylon 6 (a) and nylon 6,6 (b)

the change in the physical interaction between the hydrocarbon rubber phase and the polyamide matrix phase (manifested at the interface) is at the root of the decrease in particle size with CH_2/NHCO ratio for the nylon *x*,*y*-based blends shown in *Figure 7*. The purpose here is to explore this proposal in a quantitative way.

We believe that the nature of the interface affects the morphology in two ways. First, the magnitude of the polymer–polymer interaction energy at the interface (equation (4)) influences the interfacial tension between the two phases. Second, the interaction energy also determines interface thickness (equation (3)) which controls the extent of reaction possible in the interfacial zone. It is believed that these interrelated issues can play a pivotal role in the determination of final morphology in reactive blends.

As pointed out earlier, because of the difficulties involved in the direct measurement of interfacial tension in molten polymer systems[31,32], several theoretical frameworks have been proposed for obtaining a quantitative value for this parameter. In this section we shall use the model proposed by Helfand[27–29] to evaluate the interfacial parameters shown in equations (3) and (4). In order to do this, it is first necessary to have information about the interaction energy density, B, for this system. This is possible by making certain assumptions. First, we assume that the styrenic phase in the triblock copolymer, SEBS, does not play a significant role in the interaction between the two phases. Second, we assume that the midblock composed of ethylene–butene units can be modelled as a structure composed of CH_2 groups. Third, we model the aliphatic polyamides as a mix of methylene (CH_2) and amide (NHCO) units. The last assumption has been widely utilized by Ellis in his recent work[68–73] and is based on the mean-field binary interaction model proposed by several investigators[74–76]. On the basis of these assumptions, the nylon/SEBS system can be modelled as a simple case of a homopolymer/copolymer system for which the effective interaction parameter may be described by

$$B = B_{13}\phi'_1 + B_{23}\phi'_2 - B_{12}\phi'_1\phi'_2 \tag{6}$$

where B_{ij} denotes the interactions between the various units, and ϕ'_i denotes the volume fraction of each component. Subscripts 1 and 2 denote the CH_2 and the NHCO units, respectively, in the polyamide, while subscript 3 denotes the CH_2 groups in SEBS. This expression is further simplified by recognizing that in this particular case $B_{13}=0$ and $B_{12}=B_{23}$. Thus we obtain:

$$B = B_{12}[\phi'_2]^2 \tag{7}$$

Hence, this model predicts that the magnitude of the overall interaction energy density should decline with decreasing values of ϕ'_2 (or increasing CH_2/NHCO ratio). Substituting the above expression into equations (2) and (4) gives:

$$d \sim \gamma \sim \phi'_2 \tag{8}$$

and into equations (3) and (7) gives:

$$\lambda \sim 1/\phi'_2 \tag{9}$$

Table 2 lists values of ϕ'_2 calculated by a group contribution method using the individual molar volumes of amide and methylene units in the polyamide[77]. Absolute values for the interfacial parameters can be calculated for the relatively simple nylon/SEBS system if the interaction energy density parameter B_{12} (or χ_{12}) in equations (3) and (4) is known. We will use the most recent value of the segmental interaction parameter, $\chi_{12}=7.98$, given by Ellis[70,71], which corresponds to $B_{12}=81\ \text{cal cm}^{-3}$. Previously reported values[72] could also be used here without affecting the qualitative trends in the interfacial parameters. *Table 2* also shows the computed interfacial parameters for SEBS and the various nylons used in this study. The rubber particle size, $\bar{d}_w$, determined from TEM photomicrographs shown earlier and the extent of reaction in these blends are also shown. The computed interfacial tension for nylon 6,6/SEBS is in remarkably close agreement with the experimentally measured value for the nylon 6,6/polyethylene system ($10.7\ \text{mN m}^{-1}$) recently reported by Elmendorp[32]. As expected, the interfacial tension decreases while the interfacial thickness increases as the methylene content of the nylon increases.

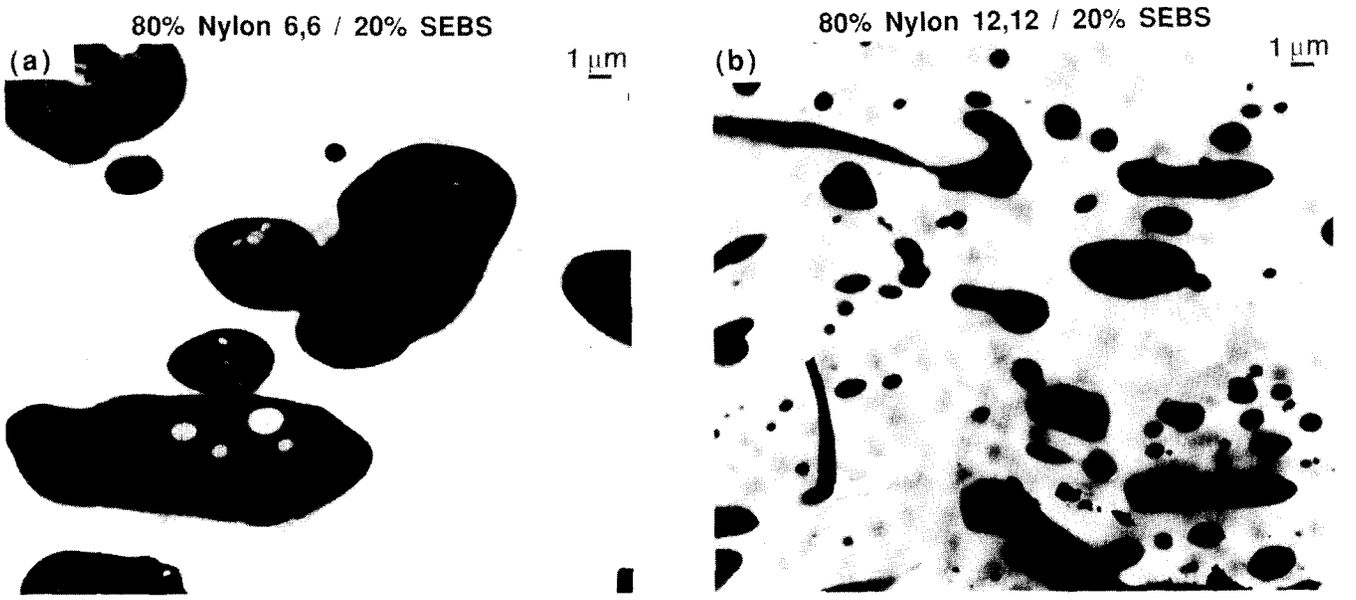

Figure 12 TEM photomicrographs of blends containing 20% SEBS and 80% (a) nylon 6,6 and (b) nylon 12,12. The rubber phase has been stained with RuO_4 in both cases

As a preliminary step towards validating the relationship proposed in equation (8), nylon 6,6 and nylon 12,12, which have widely different CH_2/NHCO ratios, were blended in a single-screw extruder with the unmaleated elastomer, SEBS. The main issue was to ascertain how accurately this model predicts the relationship between ϕ'_2 (or interfacial tension) and the particle size for this simple non-reactive system. *Figure 12* shows TEM photomicrographs for blends of nylon 12,12 and nylon 6,6 with 20% SEBS. Owing to the relatively large size of the rubber particles generated in these non-reactive systems, several TEM photomicrographs had to be analysed to measure a sufficient number of rubber particles (80–100) to obtain a statistically valid average particle size, $\bar{d}_w$. *Figure 13* shows the computed particle size *versus* the interfacial tension for these non-reactive blends. A linear fit through the origin for these data shows that the relationship proposed in equation (8) is adequately satisfied for this non-reactive system where viscosities and mixing conditions have been held fixed.

The situation for reactive blends is more complex since grafting changes the interfacial tension and shifts the balance between drop break-up and coalescence via steric stabilization. Nevertheless, it is reasonable to expect that the physical interaction at the interface is still a factor which influences particle size. If we assume that the grafting reaction between SEBS-*g*-MA and the polyamides changes the interfacial tension and the extent of steric stabilization (constant extent of grafting) by the same amount regardless of the polyamide type, then equation (8) should also remain valid for blends of nylon *x*,*y* with SEBS-*g*-MA. *Figure 14* shows the variation in the particle size for nylon *x*,*y*/SEBS-*g*-MA blends. While the plot is essentially linear, there is not a direct proportionality between the polyamide composition or the calculated interfacial tension for the polyamide/SEBS system. For example, in going from nylon 6,6 to nylon 12,12, γ is decreased roughly by a factor of 2, whereas rubber particle diameter is decreased by a factor of 4.7. This may stem from violation of the assumption that the extent of reaction is constant.

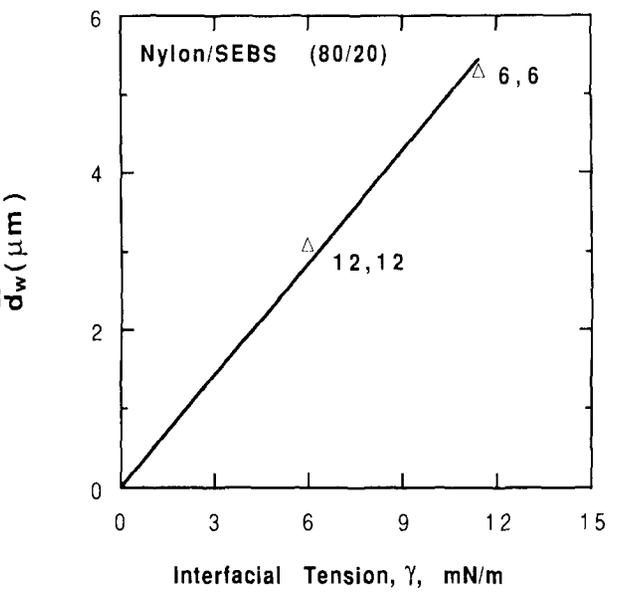

Figure 13 SEBS particle size as a function of calculated nylon *x*,*y*/SEBS interfacial tension for matched melt viscosities of the components

The fraction, x, of the original amine groups in the polyamide that were consumed during blending with SEBS-*g*-MA provides a measure of the extent of grafting. This information was obtained from amine endgroup titration of each original polyamide and its blend with SEBS-*g*-MA. *Table 2* shows the extent of reaction after blending for the various polyamides. Only those polyamides that had viscosities closely matched to the viscosity of the SEBS-*g*-MA were examined in this way. As seen in *Table 2*, the extent of reaction remains relatively constant among the nylon x series but increases remarkably with the CH_2/NHCO ratio for the nylon *x*,*y* series. The extent of reaction should depend on the breadth of the polyamide–rubber interface since this controls the access of reactive groups to each other, per unit area of the interface, as suggested by the schematic illustration in *Figure 15*. It should also depend on the

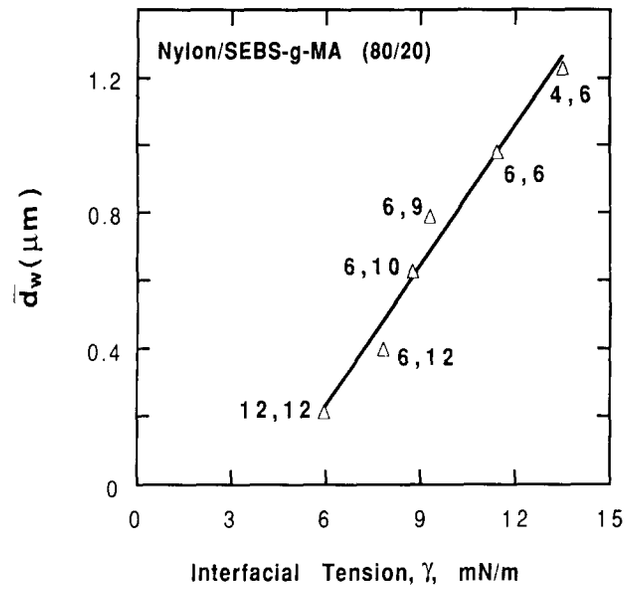

Figure 14 SEBS-*g*-MA particle size as a function of nylon *x*,*y*/SEBS interfacial tension

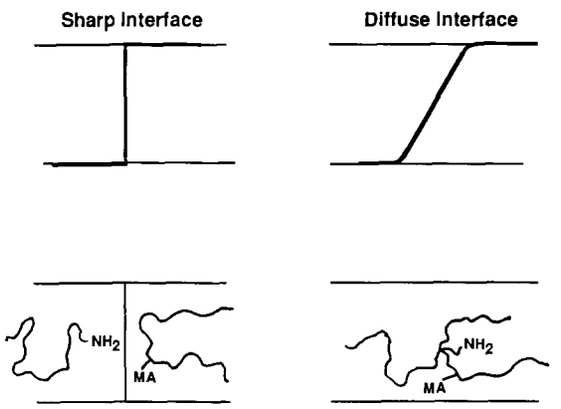

Figure 15 Schematic illustration of sharp and diffuse interfaces in polyamide/SEBS-*g*-MA blends. When reactive groups in different phases can co-exist in an interfacial zone, opportunity for reaction increases relative to a sharp interface

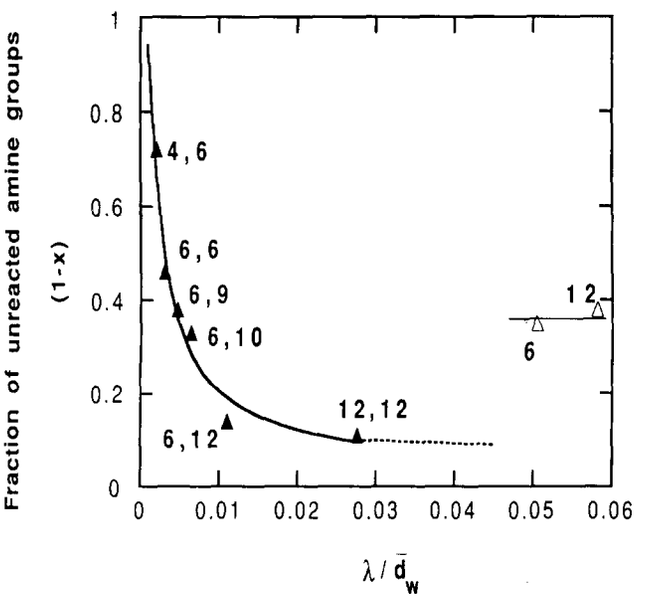

Figure 16 Fraction of unreacted amine groups *versus* estimated factor proportional to interfacial volume fraction for monofunctional and difunctional polyamides

amount of interfacial area generated during blending. For simple spherical particles of radius R, the surface area per volume of particles is proportional to $1/R$ (or $1/d$). Thus, for an interface of thickness λ, the volume fraction of the interfacial region should be approximately proportional to λ/d. *Figure 16* shows the fraction of amine groups that have not reacted *versus* λ/d, which is proportional to the interface volume fraction prior to any reaction (where for d we use $\bar{d}_w$ deduced from TEM photomicrographs). For the difunctional polyamides, a larger volume fraction of interfacial region allows the functional groups greater access to one another and apparently leads to a higher extent of reaction. This in turn further lowers the interfacial tension and increases steric stabilization, which leads to a greater change in the rubber particle size of these reactive blends, as the CH_2/NHCO ratio is varied, than that predicted from solely physical considerations. Of course, the above analysis is rather an approximation since the rubber particles of interest are far from spherical, but their similarity within the nylon *x*,*y* series should allow the trend to be maintained.

For the monofunctional polyamide blends, on the other hand, there is little change either in the extent of reaction or the available interfacial volume fraction ($\lambda/\bar{d}_w$) as shown in *Figure 16*. We believe that this may stem from the more efficient steric stabilization that results from the single-end grafting of nylon *x* chains to the SEBS-*g*-MA particles. This leads to very small particles and a high interfacial area but may also limit the access of unreacted chains to the interface, thus setting an upper limit on the extent of reaction possible. In spite of a much larger interfacial zone, the extent of reaction for the nylon *x* materials with SEBS-*g*-MA is lower than that observed for some blends based on nylon *x*,*y* with high CH_2/NHCO ratios.

Clearly, the combination of physical and chemical events involved in the morphology generation of these reactive blends is very complex. The above arguments do not explain all the observations in detail but we feel that several important issues have been identified and quantified to the extent possible at this time.

CONCLUSIONS

There is a fundamental difference in the morphology generated when monofunctional and difunctional polyamides are blended with a maleated elastomer in a single-screw extruder. The one-point attachment for the monofunctional polyamides leads to the formation of small spherical particles of SEBS-*g*-MA whose diameter remains virtually unchanged when the CH_2/NHCO ratio is varied in the nylon *x* series. This is believed to stem from the steric stabilization which is created by such a configuration. The difunctional polyamides, on the other hand, yield much larger and more complex-shaped particles whose size steadily decreases with increasing CH_2/NHCO ratio in the nylon *x*,*y* series. The latter has been attributed to changes in the physical interaction between the two phases as the methylene content in the polyamide repeat unit is varied that, among other things, lead to a change in the extent of reaction with the maleated rubber.

Use of the maleated copolymer, SEBS-*g*-MA, has a dramatic effect on the rubber-phase particle size. Evidently the formation of graft copolymer at the

interface by reaction with the polyamide chains significantly shifts the balance between drop break-up and coalescence of rubber particles during the mixing of these blends. For the non-reactive blends, there is a steady increase in particle size with concentration of the rubber phase due to increased coalescence as predicted by various theories of morphology development[20–26]. On the other hand, for both nylon 6 and nylon 6,6, the size of SEBS-*g*-MA particles remains relatively fixed from 1 to 20% rubber content. At low rubber concentrations ($\sim 1\%$), where the rate of coalescence should be minimal, relatively large SEBS-*g*-MA particles are generated in nylon 6,6 (*Figures 8* and *9*) while small, spherical particles are observed in nylon 6. Thus, the different rubber-particle morphology observed for toughened blends of nylon 6 and nylon 6,6 exists even in dilute blends where the coalescence should be relatively unimportant. It would appear that the differences in rubber particle size caused by double-end grafting (possible in nylon *x,y* materials) *versus* single-end grafting for the type of nylon *x* materials used here stem from differences in particle drop break-up rather than differences in coalescence.

It was shown that the extent of graft reaction between SEBS-*g*-MA and members of the nylon *x,y* series increases as the CH_2/NHCO content increases. This observation can be justified based on arguments about the thickness of the rubber–polyamide interface which is one factor that governs the degree of access the functional groups have to one another for reaction. On the other hand, the extent of reaction in the nylon *x* series does not vary much with the CH_2/NHCO ratio, nor does the rubber particle size.

ACKNOWLEDGEMENTS

This research was supported by the US Army Research Office. The authors are indebted to Shell Development Company for the materials and technical communications, to A. J. Oshinski for the amine endgroup titrations and to Daniel Kallick at the University of Texas Photography Department.

REFERENCES

1 Gilmore, D. and Modic, M. J. *Soc. Plast. Eng. ANTEC* 1989, **47**, 1371
2 Modic, M. J., Gilmore, D. W. and Kirkpatrick, J. P. Proc. 1st Int. Congr. on Compatibilization and Reactive Polymer Alloying (Compalloy '89), New Orleans, LA, 1989, p. 197
3 Gelles, R., Modic, M. J. and Kirkpatrick, J. *Soc. Plast. Eng. ANTEC* 1988, **46**, 513
4 Oshinski, A. J., Keskkula, H. and Paul, D. R. *Polymer* 1992, **33**, 268
5 Oshinski, A. J., Keskkula, H. and Paul, D. R. *Polymer* 1992, **33**, 284
6 Takeda, Y., Keskkula, H. and Paul, D. R. *Polymer* 1992, **33**, 3173
7 Oostenbrink, A. J., Molenaar, L. J. and Gaymans, R. J. 'Polyamide–rubber blends: influence of very small rubber particles sizes on impact strength', Poster given at 6th Annual Meeting of Polymer Processing Society, Nice, France, 18–20 April 1990
8 Epstein, B. N. *US Pat 4 174 358* (to E.I. du Pont Co.), 1979
9 Epstein, B. N. *US Pat 4 172 859* (to E.I. du Pont Co.), 1979
10 Borggreve, R. J. M., Gaymans, R. J., Schuijer, J. and Ingen Housz, J. F. *Polymer* 1987, **28**, 1489
11 Borggreve, R. J. M. and Gaymans, R. J. *Polymer* 1989, **30**, 63
12 Gaymans, R. J. and Borggreve, R. J. M. in 'Contemporary Topics of Polymer Science', (Ed. B. M. Culbertson), Vol. 6, Plenum Press, New York, 1989, p. 461
13 Wu, S. *Polymer* 1985, **26**, 1855
14 Min, K., White, J. L. and Fellers, J. F. *Polym. Eng. Sci.* 1984, **24**, 1327
15 Wu, S. *Polym. Eng. Sci.* 1987, **27**, 335
16 Serpe, G., Jarrin, J. and Dawans, F. *Polym. Eng. Sci.* 1990, **30**, 553
17 Favis, B. D. and Chalifoux, J. P. *Polym. Eng. Sci.* 1987, **27**, 1591
18 Mason, C. D., Yoang, J. A., Haylock, J. C. and Twilley, I. C. *US Pat. 4 945 129* (to Allied Signal, Inc.), 1990
19 Majumdar, B., Keskkula, H. and Paul, D. R. *Polymer* 1994, **35**, 1399
20 Taylor, G. I. *Proc. R. Soc. (London) (A)* 1932, **138**, 41
21 Taylor, G. I. *Proc. R. Soc. (London) (A)* 1934, **146**, 501
22 Von Smoluchowski, M. *Z. Physik. Chem.* 1917, **92**, 129
23 Von Smoluchowski, M. *Physik. Z.* 1916, **17**, 557, 585
24 Tokita, N. *Rubber Chem. Technol.* 1977, **50**, 292
25 Elmendorp, J. J. and Van der Vegt, A. K. *Polym. Eng. Sci.* 1986, **26**, 1332
26 Fortelny, I. and Kovar, J. *Polym. Compos.* 1988, **9**, 119
27 Helfand, E. *J. Chem. Phys.* 1975, **62**, 999
28 Helfand, E. and Sapse, A. M. *J. Chem. Phys.* 1975, **62**, 1327
29 Helfand, E. and Tagami, Y. *J. Chem. Phys.* 1972, **56**, 3592
30 Roe, R. J. *J. Chem. Phys.* 1975, **62**, 490
31 Wu, S. 'Polymer Interface and Adhesion', Marcel Dekker, New York, 1982
32 Elmendorp, J. J. and Vos, G. D. *Polym. Eng. Sci.* 1986, **26**, 415
33 Anastasiadis, S. H., Gancarz, I. and Koberstein, J. T. *Macromolecules* 1988, **21**, 2980
34 Anastasiadis, S. H., Chen, J. K., Koberstein, J. T., Siegel, A. F., Sohn, J. E. and Emerson, J. A. *J. Colloid Interface Sci.* 1987, **119**, 55
35 Anastasiadis, S. H., Chen, J. K., Koberstein, J. T., Sohn, J. E. and Emerson, J. A. *Polym. Eng. Sci.* 1986, **36**, 1410
36 Callaghan, T. A., Takakuwa, K., Paul, D. R. and Padwa, A. R. *Polymer* accepted for publication
37 Brandrup, J. and Immergut, E. H. (Eds) 'Polymer Handbook' 3rd edn, John Wiley, New York, 1989
38 Shull, K. R., Kramer, E. J., Hadziioannou, G. and Tang, W. *Macromolecules* 1990, **23**, 4780
39 Shull, K. R. and Kramer, E. J. *Macromolecules* 1990, **23**, 4769
40 Leibler, L. *Makromol. Chem., Macromol. Symp.* 1988, **16**, 1
41 Noolandi, J. and Hong, K. M. *Macromolecules* 1984, **17**, 1531
42 Noolandi, J. and Hong, K. M. *Macromolecules* 1982, **15**, 482
43 Jerome, R., Fayt, R. and Teyssie, Ph. in 'Thermoplastic Elastomers: A Comprehensive Review' (Eds N. R. Legge, H. Schroeder and G. Holden), Hanser Verlag, Munich, 1987, Ch. 12, Sect. 7
44 Teyssie, Ph. *Makromol. Chem., Macromol. Symp.* 1988, **22**, 83
45 Sjoerdsma, S. D., Bleijenberg, A. C. A. M. and Heikens, D. *Polymer* 1981, **22**, 619
46 Paul, D. R. in 'Functional Polymers' (Eds D. E. Bergbreiter and C. E. Martin), Plenum Press, New York, 1989, p. 1
47 Paul, D. R., Barlow, J. W. and Keskkula, H. in 'Encyclopedia of Polymer Science and Engineering' (Eds H. F. Mark, N. Bikales, C. G. Overberger and G. Menges), Wiley-Interscience, New York, 2nd Edn, 1988, Vol. 12, p. 399
48 Paul, D. R. in 'Thermoplastic Elastomers: Research and Development' (Eds. N. R. Legge, H. Schroeder and G. Holden), Hanser Verlag, Munich, 1987, Ch. 12, Sect. 6
49 Paul, D. R. and Newman, S. (Eds) 'Polymer Blends', Vols I and II, Academic Press, New York, 1978
50 Willis, J. M., Favis, B. D. and Lunt, J. *Polym. Eng. Sci.* 1990, **30**, 1073
51 Trent, J. S. *Macromolecules* 1984, **17**, 2930
52 Trent, J. S., Scheinbeim, J. I. and Couchman, P. R. *Macromolecules* 1983, **16**, 589
53 Trent, J. S., Scheinbeim, J. I. and Couchman, P. R. *J. Polym. Sci., Polym. Lett. Edn* 1981, **19**, 315
54 Vitali, R. and Montani, E. *Polymer* 1980, **21**, 1220
55 Martinez-Salazar, J. and Cannon, C. G. *J. Mater. Sci. Lett.* 1984, **3**, 693
56 Morel, D. E. and Grubb, D. T. *Polymer* 1984, **25**, 41
57 Boylston, E. K. and Rollins, M. L. *Microscope* 1971, **19**, 255
58 Spit, B. J. *Faserforsch. Textiltech.* 1967, **18**, 161
59 Rusnock, J. A. and Hansen, D. *J. Polym. Sci. Part A* 1965, **3**, 617
60 Irani, R. R. and Callis, C. F. 'Particle Size: Measurement, Interpretation and Application', Wiley, New York, 1963
61 Chamot, E. M. and Mason, C. W. 'Handbook of Chemical Microscopy', Wiley, London, 1983
62 Bach, G. 'Qualitative Methods in Morphology', Springer Verlag, Berlin, 1967
63 Mihira, K., Ohsawa, T. and Nakayamu, A. *Kolloid. Z.* 1968, **222**, 135

64 Triacca, V. J., Ziaee, S., Barlow, J. W., Keskkula, H. and Paul, D. R. *Polymer* 1991, **32**, 1401
65 Barlow, J. W., Shaver, G. P. and Paul, D. R. Proc. 1st Int. Congr. on Compatibilization and Reactive Polymer Alloying (Compalloy '89), New Orleans, LA, 1989, p. 221
66 Fowler, M. W. and Baker, W. E. *Polym. Eng. Sci.* 1988, **28**, 1427
67 Baker, W. E. and Saleem, M. *Polymer* 1987, **28**, 2057
68 Ellis, T. S. *Macromolecules* 1991, **24**, 3845
69 Ellis, T. S. *Macromolecules* 1990, **23**, 1494
70 Ellis, T. S. *Polymer* 1990, **31**, 1058
71 Ellis, T. S. *Polym. Eng. Sci.* 1990, **30**, 998
72 Ellis, T. S. *Macromolecules* 1989, **22**, 742
73 Ellis, T. S. *Polymer* 1988, **29**, 2015
74 Paul, D. R. and Barlow, J. W. *Polymer* 1984, **25**, 487
75 ten Brinke, G., Karasz, F. E. and MacKnight, W. J. *Macromolecules* 1983, **16**, 1827
76 Kambour, R. P., Bendler, J. T. and Bopp, R. C. *Macromolecules* 1983, **16**, 753
77 Van Krevelen, D. W. 'Properties of Polymers', Elsevier, New York, 1976